sustainability

Article

Feasibility Analysis of Indirect Evaporative Cooling System Assisted by Liquid Desiccant for Data Centers in Hot-Humid Regions

Wenchao Shi [1], Xiaochen Ma [1], Yunran Min [2,*] and Hongxing Yang [1]

[1] Renewable Energy Research Group (RERG), Department of Building Environment and Energy Engineering, The Hong Kong Polytechnic University, Hong Kong, China
[2] College of Marine Equipment and Mechanical Engineering, Jimei University, Xiamen 361021, China
* Correspondence: minyunran@jmu.edu.cn

Abstract: The rapid development of data centers (DCs) has led to a marked increase in energy consumption in recent years, which poses a direct challenge to global efforts aimed at reducing carbon emissions. In regions with hot and humid climates, the energy demand is largely driven by air conditioning systems necessarily to maintain appropriate operational temperatures. This study proposes a novel multi-stage indirect evaporative cooling (IEC) system, incorporating a liquid desiccant in the primary air channel to address the cooling demands of such DCs. Our approach involves a two-stage process where the first stage uses a liquid desiccant-based IEC (LD-IEC) for air dehumidification and the second stage utilizes the treated air from the first stage as the secondary air to enhance the cooling effect. A simulation model of the proposed system is established with validation, and the performance of the multi-stage system was also discussed based on different operation modes. Furthermore, a case study was conducted to investigate the feasibility of using this system in the DC under a typical hot and humid zone. The findings reveal that the first-stage LD-IEC is capable of diminishing the wet-bulb temperature of the ambient air. Furthermore, the case study demonstrates that the proposed system can greatly improve the temperature drop by 72.7% compared to the single IEC, which noticeably reduces the operation time of energy-intensive supplementary cooling equipment from 5092 h to 31 h given the supply air temperature threshold of 25 °C. In summary, the proposed system could substantially decrease reliance on traditional cooling systems, which demonstrates a promising avenue to fully use this passive cooling technology for cooling DCs.

Keywords: air conditioning; indirect evaporative cooling; data center; liquid desiccant

Citation: Shi, W.; Ma, X.; Min, Y.; Yang, H. Feasibility Analysis of Indirect Evaporative Cooling System Assisted by Liquid Desiccant for Data Centers in Hot-Humid Regions. *Sustainability* **2024**, *16*, 2011. https://doi.org/10.3390/su16052011

Academic Editor: Ying Sheng

Received: 11 January 2024
Revised: 17 February 2024
Accepted: 26 February 2024
Published: 29 February 2024

1. Introduction

As stated by the most recent Sixth Assessment Report from the United Nations Intergovernmental Panel on Climate Change (IPCC), capping global warming to 1.5 °C will require a significant shift towards zero- or low-carbon sources for nearly all electricity generation by 2050 [1]. This transition would involve embracing renewables, fossil fuels with carbon capture and storage technology, and increased electrification of energy demand. In addition to transforming existing energy systems, reducing energy use in economies is important as well to relieve the pressure on the supply side, which is conducive to carbon peaking and neutrality [2].

As one of the major energy consumers, buildings have received significant attention in the context of dual carbon goals [3,4]. In China, the urbanization rate has shifted from rapid growth to steady growth, resulting in a gradual slowdown in the development pace of new residential and commercial buildings. However, data centers (DC), which are more important in the digital age, become a rapidly growing type of building. They link a large number of computing resources and storage resources together and are the center of massive data computing, exchange, and storage [5,6]. Nowadays, various activities, online communications, entertainment, and knowledge generation and spread increasingly rely on the internet. The increasing demand for timely interaction through the Internet has led to a sharp increase in human demand for DCs [7]. Therefore, the scale of DCs is becoming larger, the computational complexity is constantly increasing, and the structure is becoming more and more precise. However, the expansion of DCs is associated with significant energy demands, with the cooling systems alone accounting for approximately 40% of the total electricity consumption [8]. As devices progress, electronic devices are capable of delivering enhanced computational performance while also generating increased heat dissipation. Therefore, it is imperative to give due attention to both cooling and thermal management aspects [9,10], while a high percentage of cooling energy consumption obviously runs counter to dual-carbon goals.

To lessen the energy consumption of cooling systems in data rooms, researchers have focused on how to take full advantage of natural cooling, extend the operating time of natural cooling approaches, and reduce the working time of the mechanical vapor compression system (MVCS). Indirect evaporative cooling (IEC) is one of the emerging air conditioning (AC) approaches [11–13]. Figure 1 illustrates a cross-flow IEC system wherein the primary air stream to be cooled flows perpendicular to the secondary air stream that facilitates evaporation. In this configuration, the secondary air flows vertically and is in direct contact with water within the heat exchanger. As the air flows through the secondary air channel, due to the gradient in moisture content between the water film and air, water evaporation occurs and removes the latent heat. Then, the sensible heat from the primary air transfers to the secondary air stream, which is then vented externally. This approach enables the air cooling process to maintain the same humidity level and effectively prevents cross-contamination [14–16]. Furthermore, this system circumvents energy-intensive compressors or environmentally hazardous refrigerants. The air conditioning process relies on a natural phenomenon, namely the evaporation of water, with the system's main energy consumption stemming from the operation of fans and the pump. As a result, the COP and energy consumption of the IEC system are lower than those of traditional air conditioning systems, which also correlates with reduced carbon emissions [17,18].

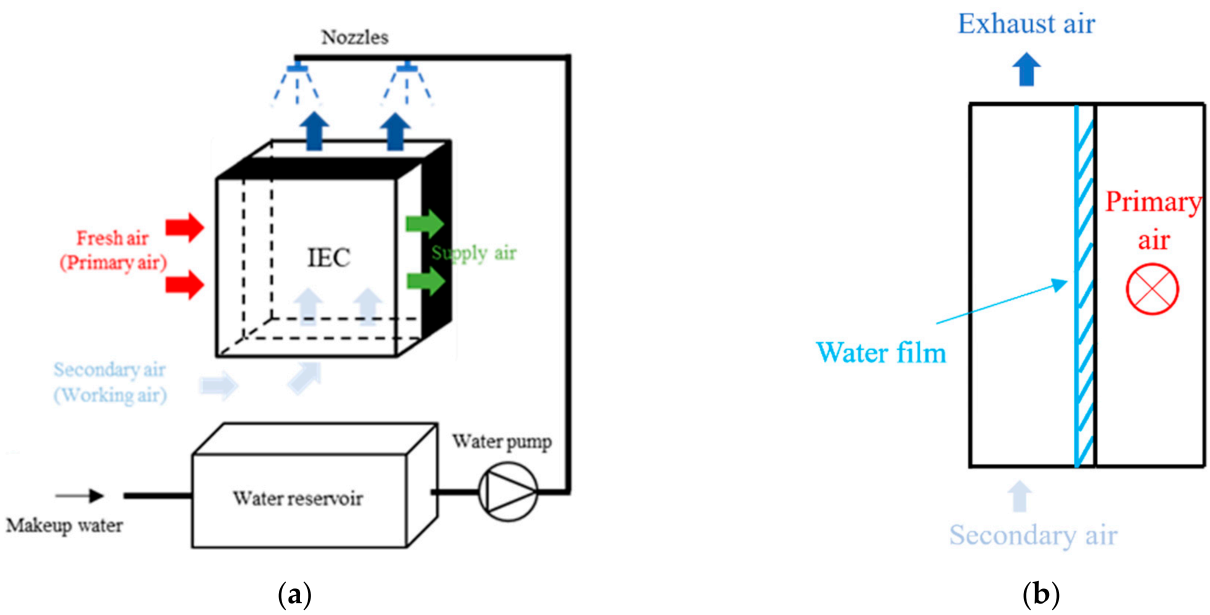

Figure 1. (**a**) Configuration of an IEC system, (**b**) side view of the IEC.

2. Literature Review

Over the past decades, fruitful research has been conducted. At the heat exchanger level, advancements have been made in both novel structures and optimal water spraying.

For instance, De Antonellis et al. evaluate the effect of spraying nozzle locations and airflow orientations on the cooling capacity of an IEC system [12]. Baffles were incorporated into the channel surface to create a small internal vortex, thereby enhancing the heat transfer coefficient [15]. Sun et al. developed a ceramic-based tubular IEC model and fabricated a prototype to test its performance under intermittent spraying [19]. Shi et al. proposed a novel IEC with porous secondary air channel surfaces to enhance the water absorbent ability and implemented periodic spraying modes to minimize operational energy consumption [20]. Corrugated channels were designed and produced to increase the contact area in comparison to traditional IECs [21]. Ahmed et al. assessed the external, internal, and mixed spraying modes for the same IEC under varying inlet conditions, identifying the internal spraying plan as a reliable method to improve mass transfer in the hexagonal IEC [22]. After evaluating six configurations, they recommended a top or a horizontal spraying scheme for optimal water distribution.

At the system level, hybrid IEC systems have been developed to meet cooling requirements and decrease energy consumption. Wan et al. evaluated the IEC system integrated with a paraffin-based phase change material (PCM) under commercial operating conditions. The use of PCMs shifts the peak load and enables a higher temperature of the chiller water [23]. Nemati et al. proposed to precool the air by the ground source heat exchanger and further cool the supply air through the IEC, which resulted in a 45% reduction in water consumption [24]. Shi et al. performed a techno-economic evaluation of a dedicated outdoor air system using an IEC and an auxiliary cooling coil in an office building. Their findings underscore the viability of extending IEC applications in regions characterized by hot and humid climates [25]. Chen et al. incorporated an IEC into a mechanical vapor compression system to partially undertake the cooling load, reducing the energy consumption by at least 19% [26]. Yan et al. proposed a DXAC-IEC system with an adaptive controller and evaluated the performance under hot and arid climates, which saved 27.7% of energy during the transition season compared to the standalone IEC [27]. Tripathi and Kumar et al. investigated a tubular IEC system powered by solar photovoltaic panels under various inlet conditions in a hot and arid city in India [28]. Hu et al. proposed a novel synergy between IEC and radiative cooling, which obtained an 11.9% improvement in dew-point effectiveness and superior cooling performance in dry climates [29].

Since the load in the DC is mainly from equipment heat dissipation, the proportion of sensible heat is extremely high. The handling of sensible heat loads is a key feature and advantage of IECs. Consequently, in recent years, projects in hot and arid areas have begun to incorporate direct evaporative cooling (DEC) and IEC in the DC's AC system, which have received noticeable energy saving benefits [30–32]. The implementation of the DEC for fresh air at the Facebook DC achieves significant energy savings in Plinville, a dry region in the USA [33]. Kao Data in London yielded an average PUE of 1.21 at a full IT load by incorporating an IEC in its AC infrastructure [34]. Yan et al. performed multi-objective optimizations of a counterflow IEC for DCs under hot and dry climate conditions based on response surface methodology [35]. Cui et al. analyzed the climatic applicability of a single-stage IEC with mechanical cooling for DCs in China. Results show sufficient cooling in western arid regions, while supplementary cooling is necessary with a prolonged operation period in hot and humid regions [36].

From the literature above, despite these successes in the application of IEC technology in DCs of arid regions, some research gaps still remain to be addressed, especially in hot and humid regions. Firstly, due to the high humidity of ambient air, evaporation is constrained so that the cooling effect will be noticeably reduced, and this is the main reason why IEC technology is yet to be adopted in DCs of such areas. Secondly, the cooling performance of an IEC system through the addition of a liquid desiccant to overcome geographical limitations in hot and humid areas has not been quantitatively detailed. Thirdly, the system feasibility remains to be analyzed based on the local weather profile of a typical hot-humid region.

In response to these gaps, this study proposed a novel multi-stage IEC system tailored for a DC situated in hot-humid regions. A simulation model was established with validation, and the cooling performance of the system was investigated under a variety of conditions through parametric analysis. Then, a case study was performed to assess the viability of the hybrid system in a typical hot-humid area (Hong Kong), indicating a potential approach to lessen the reliance on traditional AC systems and fully use passive cooling technology for DC cooling in similar climatic conditions. The limitations and future works are summarized as well to guide the further research steps.

3. Methodology

3.1. System Configuration

As illustrated in the Section 1, the evaporative cooling process is inherently constrained by climatic conditions. Particularly in the summer months, the ambient outdoor relative humidity tends to be substantially elevated when the cooling requirement intensifies. Typically, both the primary air and secondary air are derived from outdoor air in an IEC. The secondary air is intended to facilitate evaporation upon contact with the water through the humidity difference with the saturated liquid surface. Nonetheless, in hot and humid regions, the relative humidity during summer can be so high that it sometimes reaches 100%, at which point the evaporation process in the IEC becomes very difficult. This impediment can lead to a cooling output that fails to satisfy the requisite standards for thermal management. To mitigate this limitation and procure drier air for an improved cooling effect, this study proposes a multi-stage evaporative cooling system tailored for DC applications. The proposed system encompasses a liquid-desiccant-based (LD) IEC, a conventional IEC, and an auxiliary cooling section to fulfill the cooling demand. In DCs, there is typically no need for fresh air, or a separate AC system is responsible for handling outdoor fresh air and delivering it to specific personnel areas. The hot air produced by the electronic devices is handled using AC equipment and circulated. The schematic diagram of the airflow configuration used in a DC is shown in Figure 2. The LD-IEC and the normal IEC are made of a metal material with good anti-corrosion. In summer (Figure 2a), liquid desiccant dehumidification is needed to reduce the humidity of outdoor air so that evaporation can happen under a larger gradient in the secondary air channel. The outdoor fresh air passes the LD-IEC as primary air, and the liquid solution is sprayed into the primary air channel to dehumidify moist fresh air. The primary outlet air from LD-IEC is divided into two air streams. Air stream 1 is delivered to the second-stage IEC as secondary air, while air stream 2 is introduced to the secondary air channel of the first-stage LD-IEC. As air stream 2 has been dehumidified, it can result in a greater humidity differential between it and the water film on the secondary channel, which enhances the evaporation process. This, in turn, contributes to a decrease in the temperature of the total air stream in the primary air channel compared to the situation without dehumidification and removes some latent heat released during the dehumidification process. After passing through the secondary air channel and aiding in the evaporation process, air stream 2 is discharged into the ambient environment at the exit. Then, the circulated hot air from the DC can be cooled when it is passing the primary air channel of the second-stage IEC. To ensure that the supply air temperature is able to cool the electronic device in the DC, a supplementary cooling section is positioned after the second-stage IEC. In spring and autumn (Figure 2b), only the second-stage IEC needs to operate, and the on/off status of the water spraying depends on the supply air temperature and weather conditions.

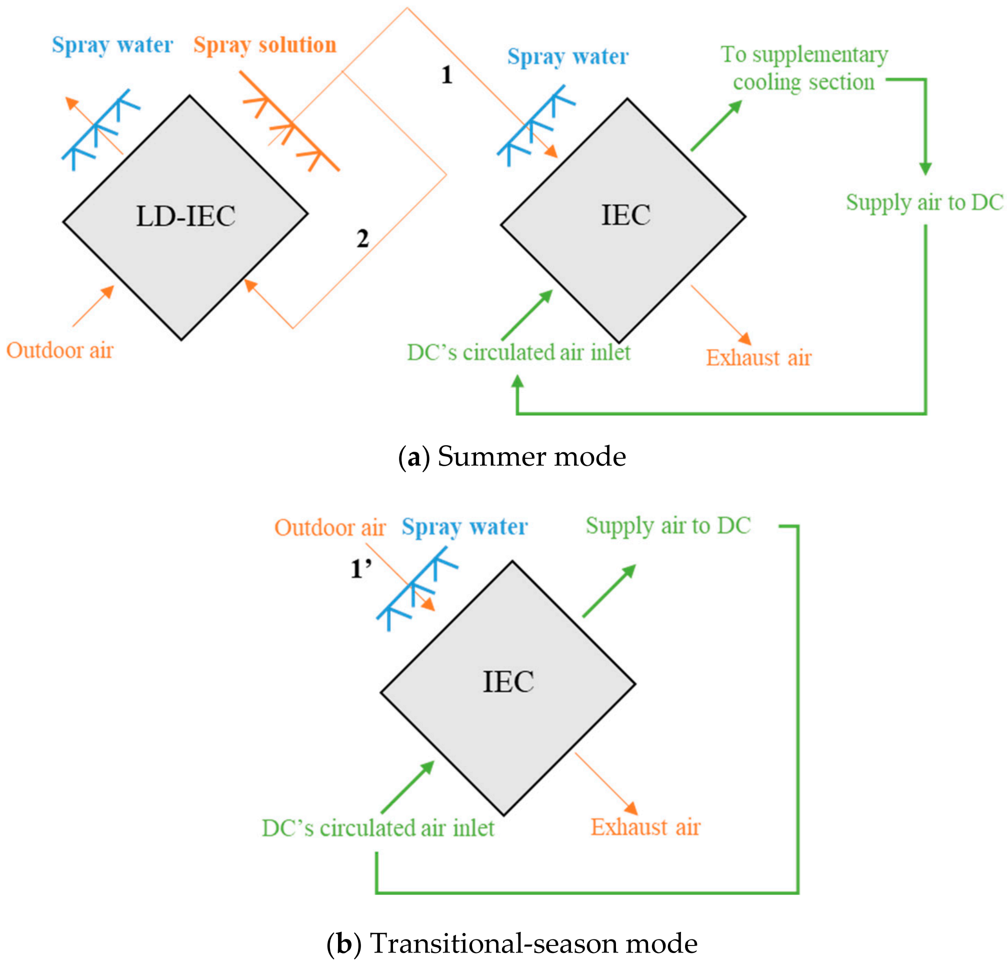

Figure 2. Schematic diagram of the multi-stage evaporative cooling system used for a DC. 1: First-stage LD-IEC outlet primary air as second-stage IEC secondary air. 2: First-stage LD-IEC outlet primary air as its secondary air. 1′: Outdoor air as secondary air of IEC.

3.2. Model Establishment

To facilitate the modeling of the aforementioned air conditioning (AC) devices, it is imperative to delineate certain assumptions, which are also widely endorsed in existing literature [37,38] as follows: (1) The external environment is considered to be isolated from the LD-IEC/IEC, negating any heat or mass exchange with the surroundings; (2) Both air and water are treated as incompressible fluids in steady state; (3) Due to their small *Re* number, the states of the fluids can be considered as laminar flow; (4) Thermal resistance of the thin channel sheet and the liquid membrane is negligible because their tiny thickness; (5) The solution and water are distributed uniformly over the whole of the passages; (6) The desiccant solution is maintained at a consistent concentration, with the potential for regeneration via a heat source such as solar energy; (7) The heat and mass transfer occur solely along the fluid's flow direction.

3.2.1. IEC Model

The 2D numerical model of the IEC has been developed according to the general assumptions outlined in our previous study, and the essential equations are briefly summarized as follows. The core equations that govern the behavior of the secondary air and its interaction with the water membrane are expressed from Equations (1)–(3):

$$h_s(t_w - t_s)\cdot dxdy + h_{fg}h_{ms}(\omega_{t_w} - \omega_s)dxdy = \dot{m}_s\frac{\partial i_s}{\partial y}dy \quad (1)$$

$$h_{ms}(\omega_{s,\,sat} - \omega_s) \cdot dxdy = m_s \frac{\partial \omega_s}{\partial y} \cdot dy \tag{2}$$

$$\dot{m_s} = \frac{dx}{L} m_s \tag{3}$$

The heat transfer equation for the primary air is:

$$h_p (t_p - t_w) \cdot dxdy = c_{pa} \dot{m_p} \frac{\partial t_p}{\partial y} dx \tag{4}$$

$$\dot{m_p} = \frac{dy}{H} m_p \tag{5}$$

The energy balance can be written as:

$$\dot{m_s} \frac{\partial i_s}{\partial y} - c_{pa} \dot{m_p} \frac{\partial t_p}{\partial x} = c_{pw} t_{ew} \frac{\partial m_e}{\partial y} \tag{6}$$

$$\frac{\partial m_e}{\partial y} = \dot{m_s} \frac{\partial w_s}{\partial y} \tag{7}$$

The convective heat and mass transfer coefficients are connected through the Lewis number, as shown in Equation (8) [39], while the convective heat transfer coefficient is correlated with the Nusselt number, as seen in Equation (9).

$$Le^{\frac{2}{3}} = \frac{h_s}{h_{ms} c_{pa}} \tag{8}$$

$$h = \frac{Nu \cdot \lambda}{d_e} \tag{9}$$

$$Nu = 0.664 Re^{\frac{1}{2}} Pr^{\frac{1}{3}} \tag{10}$$

where the Lewis number is determined as 1 [40]; c_{pa} = 1.005 kJ/(kg·°C).

The saturated humidity ratio of the interface of the liquid film and secondary air is formulated by Equation (12) [18]:

$$ln(P_{sat}) = \frac{e_1}{t_w} + e_2 + e_3 t_w + e_4 {t_w}^2 + e_5 {t_w}^3 + e_6 \ln(t_w) \tag{11}$$

$$w_{s,\,sat} = 0.622 \frac{P_{sat}}{P_{atm} - P_{sat}} \tag{12}$$

where: e_1 = 5800.2206; e_2 = 1.3914993; e_3 = -0.04860239; e_4 = 4.1764769×10^{-5}; e_5 = $-1.4452093 \times 10^{-5}$; e_6 = 6.5459673; P_{atm} = 101.325 kPa; and t_w is the water film temperature, °C.

3.2.2. LD-IEC Model

For the LD-IEC, the liquid desiccant is dispersed into the primary air channel to extract water vapor from the humid air. Thus, Equations (13) and (14) are added to characterize the gradient of the moisture content, and the new energy balance formula is written as Equation (15). The equations to illustrate the heat and mass transfer in the secondary air channel are identical to that shown in the IEC model in Section 3.2.1. A lithium chloride solution, as a common desiccant material, is utilized in this study. The dehumidification of the moist air is driven by the vapor pressure difference between the air–solution interface and the main moist air stream. The equilibrium vapor pressure on the desiccant solution film surface is a function of both its temperature and concentration. Based on the thermodynamic properties acquired from published studies [41], the equilibrium vapor pressure and corresponding moisture content at the liquid desiccant interface within the primary air channel can be obtained through Equations (16) and (17).

$$h_{mp}(\omega_{sol} - \omega_p) \cdot dxdy = \dot{m}_p \frac{\partial \omega_p}{\partial x} \cdot dx \tag{13}$$

$$-\dot{m}_p \frac{\partial \omega_p}{\partial x} = \frac{\partial m_d}{\partial y} \tag{14}$$

$$\dot{m}_s \frac{\partial i_s}{\partial y} - \dot{m}_p \frac{\partial i_p}{\partial x} = c_{pw} t_{ew} \frac{\partial (m_e)}{\partial y} + c_{pw} t_{dw} \frac{\partial (m_d)}{\partial y} \tag{15}$$

$$P_{sol} = C_1 + C_2 t_{sol} + C_3 \sigma + C_4 {t_{sol}}^2 + C_5 \sigma^2 + C_6 t_{sol} \sigma \tag{16}$$

where $C_1 = -1.004$; $C_2 = 0.1265$; $C_3 = 5.982$; $C_4 = 0.003644$; $C_5 = 11.13$; $C_6 = -0.7975$; t_{sol} is the solution film temperature, °C; σ is solution concentration; and $c_{pw} = 4.18$ kJ/(kg·°C).

$$w_{sol} = 0.622 \frac{P_{sol}}{P_{atm} - P_{sol}} \tag{17}$$

where t_{sol} is the solution temperature within the range from 20 to 50 °C in Equation (13), and the solution concentration (σ) is limited within the range from 0.20 to 0.40 to avoid crystallization [42].

Referring to the system configuration in Figure 2, the boundary conditions of the first-stage LD-IEC and the second-stage IEC models are listed as follows. For the LD-IEC: $t_{p,in,LD-IEC} = t_{amb}$; $w_{p,in,LD-IEC} = w_{amb}$; $m_{p,in,LD-IEC} = m_{in,\ total}$; $t_{s,in,LD-IEC} = t_{p,out,LD-IEC}$; $w_{s,in,LD-IEC} = w_{p,out,LD-IEC}$; $m_{s,in,LD-IEC} = m_{p,in,LD-IEC}(1-r)$. For the IEC: $t_{p,in,IEC} = t_{circ,DC}$; $w_{p,in,IEC} = w_{circ,DC}$; $m_{p,in,IEC} = m_{p,LD,in} r$; $t_{s,in,IEC} = t_{p,out,LD}$; $w_{s,in,LD} = w_{p,out,LD}$; $m_{s,in,IEC} = m_{p,LD,in} r$; $r = \frac{m_{p,LD,in} - m_{s,LD,in}}{m_{p,LD,in}}$.

3.3. Model Solution and Grid Independence Monitoring

The multi-stage IEC system consists of the first-stage LD-IEC and the second-stage IEC. For the first-stage LD-IEC, we use Equations (1)–(3) and (8)–(17). For the second-stage IEC, we use Equations (1)–(12) for calculation. The finite difference method was utilized to discretize the aforementioned sets of partial differential equations into algebraic equations. Combined with the boundary conditions, MATLAB 2018b software was employed for code programing and solving. The numerical solution procedures are illustrated as follows: (1) Input air inlet conditions and geometry data (and concentration ratio and mass flow ratio for LD-IEC); (2) Calculate heat and mass transfer coefficients; (3) Assume the channel plate temperature and calculate saturated humidity; (4) Solve the governing equations of LD-IEC or IEC; (5) Figure out the new channel plate temperature, compare it with the assumed one, and judge the convergence; (6) Output the results or adjust the channel plate temperature if it cannot meet the convergence criteria. The grid number is checked to achieve a balance between accuracy and computational efficiency. As depicted in Figure 3, the variations of the results are within 0.05% when the number exceeds 140, indicating that the effect of increasing the grid number is tiny and negligible. Therefore, 140 × 140 is selected for further calculations. A threshold of 0.001 is determined as the convergence criterion.

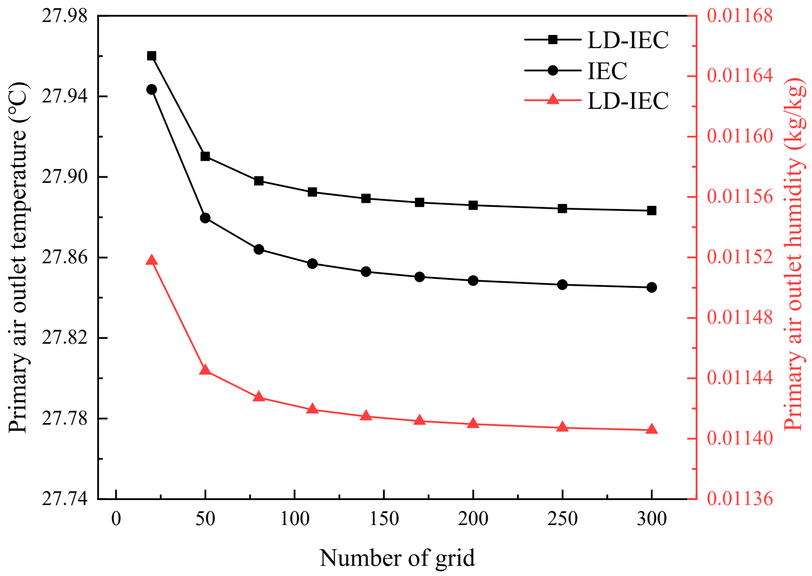

Figure 3. Outlet parameters under grid independence monitoring.

3.4. Model Validation

With respect to the model validation, the multi-stage IEC system for DC cooling has not been explicitly proposed in the existing studies so it may not be straightforwardly validated. Nonetheless, the two components in the system can be verified individually using the published results [43,44]. Comparisons between the results from the models and published studies are exhibited in Figure 4. The maximum relative deviation of the IEC primary air outlet temperature is 3.3%, while the greatest relative discrepancies of the primary air outlet temperature and humidity of the LD-IEC are −6.4% and 2.6%, respectively. These values underscore the acceptable predictive precision of the established models, thereby indicating their applicability for subsequent analysis of the proposed system for DC cooling.

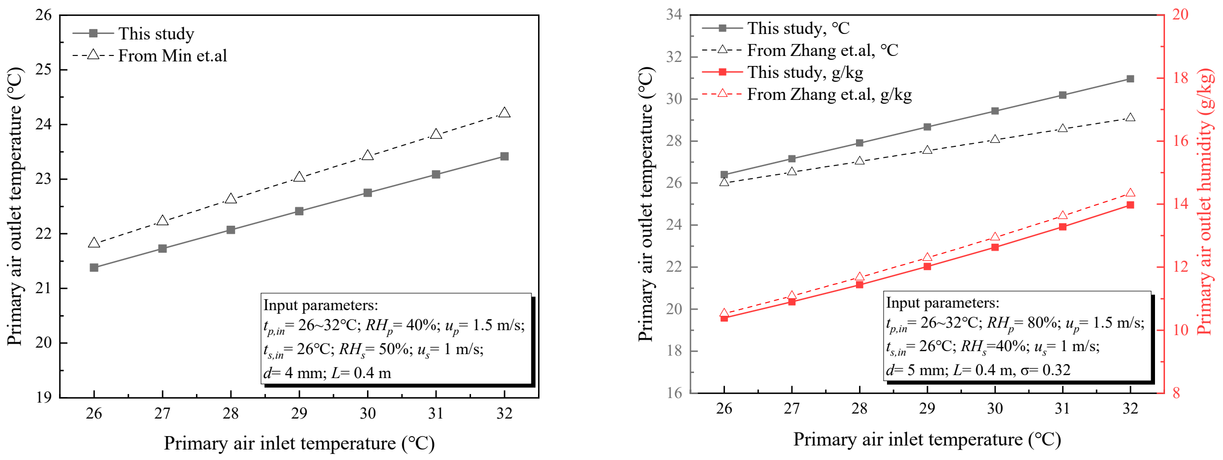

(**a**) (**b**)

Figure 4. Comparisons between the results from the present models and published research on (**a**) IEC [44], (**b**) LD-IEC [43].

4. Results and Discussions

To assess the thermal performance of the proposed multi-stage IEC system for DC cooling, the effects of essential parameters are presented. The outlet air temperature and humidity of the LD-IEC, the outlet air temperature (supply air) of the IEC, the primary air temperature drop of the IEC, and wet-bulb efficiency are illustrated in various conditions in this section. The ranges of analyzed parameters are listed in Table 1.

Table 1. Ranges of essential parameters.

Symbol (Unit)	Range	Basic Value
$t_{p,in,LD\text{-}IEC}$ (°C)	[26:2:34]	30
$RH_{p,in,LD\text{-}IEC}$ (%)	[65:5:95]	80
σ (-)	[0.2:0.05:0.4]	0.3
r (-)	[0.5:0.1:0.9]	0.7
$t_{p,in,IEC}$ (°C)	[32:2:40]	34
$u_{p,in,IEC}$ (m/s)	[2:0.5:4]	3
$m_{p,in,LD}$ = 0.003 kg/s; L = 400 mm; one channel pair for both IEC and LD-IEC		

Note: [a:b:c]: a is the start value; c is the end value; b is the interval.

4.1. Effect of Primary Air Temperature

Figure 5 delineates the impact of outdoor ambient air temperature (primary air temperature of the LD-IEC) on the thermal performance of the proposed system. A direct correlation is noticed in Figure 5a between the outdoor air temperature and the system's outlet conditions. As the outdoor air temperature rises, both the outlet temperature and humidity of the first-stage LD-IEC experience an increase. Specifically, when the outdoor air temperature at the LD-IEC inlet increases from 26 °C to 34 °C, the outlet primary air temperature and humidity of the LD-IEC increase from 23.3 °C to 30.3 °C and from 10.79 g/kg to 16.64 g/kg, respectively. In each case, there is a significant decrease in the wet-bulb temperature of the LD-IEC outlet air compared to the inlet air, decreasing from 23.3–30.9 °C to 18.1–24.3 °C.

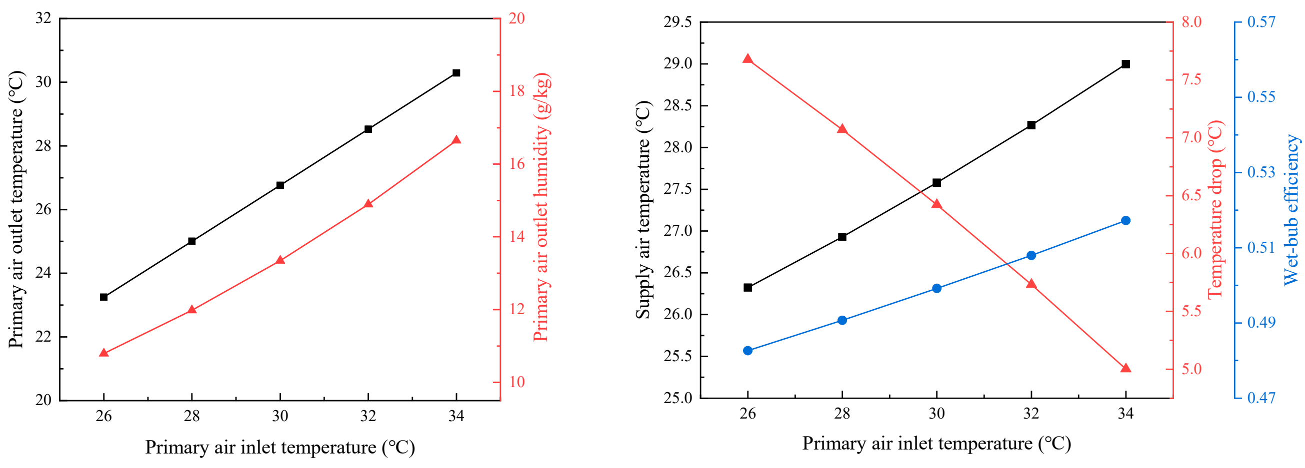

(**a**) (**b**)

Figure 5. Effect of primary air temperature on the thermal performance of (**a**) first-stage LD-IEC, (**b**) second-stage IEC.

Due to the utilization of a fraction of the LD-IEC primary air as the secondary air for the second-stage IEC, the supply air temperature (primary air outlet temperature of the IEC) increases from 26.3 °C to 29 °C. The associated temperature decrement achieved by the IEC is observed to decrease from 7.7 °C to 5.0 °C. DCs typically require the supply temperature to be controlled within the range of 18 °C to 27 °C. Consequently, when the inlet air temperature of the LD-IEC exceeds 28 °C, the proposed system fails to meet the specified supply temperature under this operating condition. An auxiliary cooling mechanism is necessitated to maintain the supply air within the prescribed thermal range. In addition, the wet-bulb efficiency of the IEC is influenced by both the primary air temperature drop of the IEC and the secondary air (i.e., outlet air status of the LD-IEC). As depicted in Figure 4b, a marginal enhancement in wet-bulb efficiency is noted with increasing inlet temperatures, with the wet-bulb efficiency ascending from 0.482 to 0.517.

4.2. Effect of Primary Air Relative Humidity

Figure 6 presents the effect of variations in the relative humidity (RH) at the inlet of the primary air on the thermal performance of the multi-stage IEC system. As the RH of the primary air increases, although the liquid desiccant can remove moisture content from the air, the overall humidity ratio increases, and the air's capacity to evaporate water diminishes, leading to a higher wet-bulb temperature and thus elevated outlet temperature and humidity after passing through the first-stage LD-IEC. As shown in Figure 6a, an escalation in the RH of the primary air from 65% to 95% at the LD-IEC inlet leads to an increase in both the temperature and humidity at the primary air outlet, with values ranging from 26.3 °C to 27.3 °C and 17.39 g/kg to 25.75 g/kg, respectively. The LD-IEC contributes to a significantly lower wet-bulb temperature compared to directly utilizing high-humidity outdoor air as the secondary air for the IEC. The wet-bulb temperature exhibits a considerable decrease from a span of 24.7 °C to 29.3 °C down to a range of 19.6 °C to 22.7 °C, indicating a more favorable potential for air cooling.

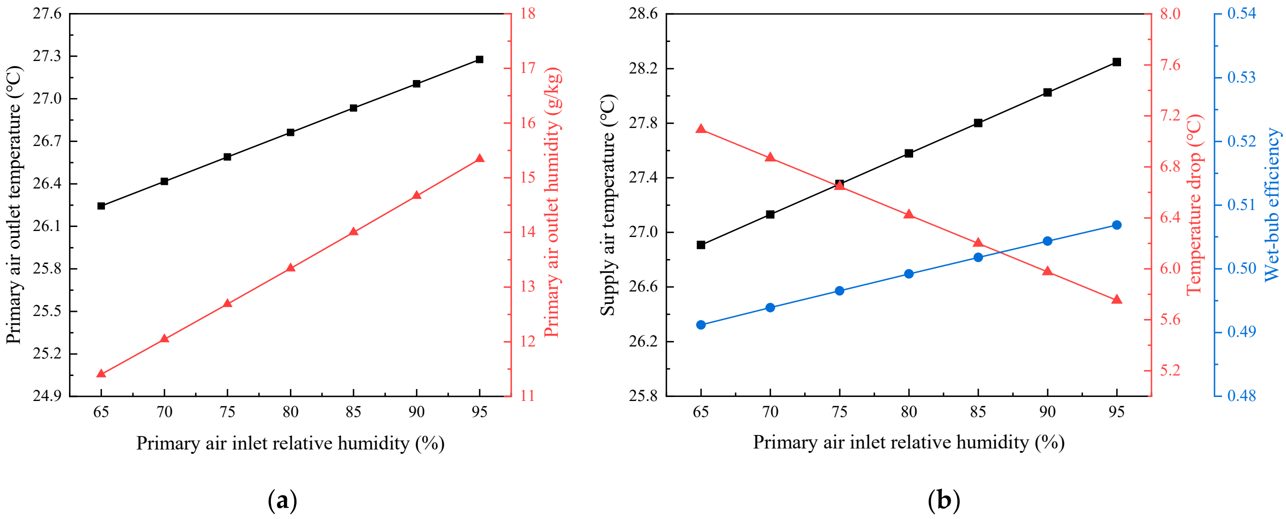

Figure 6. Effect of primary air relative humidity on the thermal performance of (**a**) first-stage LD-IEC, (**b**) second-stage IEC.

Furthermore, the increased temperature and humidity of the primary air emerging from the LD-IEC, which subsequently functions as the secondary air for the second-stage IEC, causes an upsurge in the supply air temperature from 26.9 °C to 28.3 °C. Consequently, the cooling ability of the second-stage IEC for the primary air decreases from 7.1 °C to 5.8 °C. Notably, even at an RH of 65%, the supply air temperature nears the upper threshold of 27 °C, prompting the need for an auxiliary cooling section to maintain the supply air temperature within the desired parameters. Additionally, the wet-bulb temperature of the IEC is influenced by both the temperature difference of the primary air and the secondary air conditions (i.e., outlet air temperature of the primary air from the LD-IEC in this study). As observed in Figure 6b, an increase in the RH of the air at the LD-IEC inlet results in a slight improvement in the wet-bulb efficiency, rising from 0.491 to 0.507.

4.3. Effect of Mass Flow Ratio

Figure 7 illustrates the effect of variation in the mass flow ratio (r) on the thermal performance of the proposed system. When the r value grows, the outlet temperature and humidity of the LD-IEC rise, with a steeper slope. As presented in Figure 7a, it is noticed that the higher r value from 0.5 to 0.9 corresponds to a decrease in the mass flow rate of the secondary air, resulting in greater outlet temperature and humidity of the primary air of the LD-IEC from 26.2 to 28.0 °C and from 13.13 to 13.93 g/kg, respectively. The wet-bulb temperature of the air processed by the LD-IEC ranges from 20.8 to 21.9 °C, significantly lower than the inlet wet-bulb temperature (27.1 °C), indicating a greater potential for air cooling as the secondary air for the IEC.

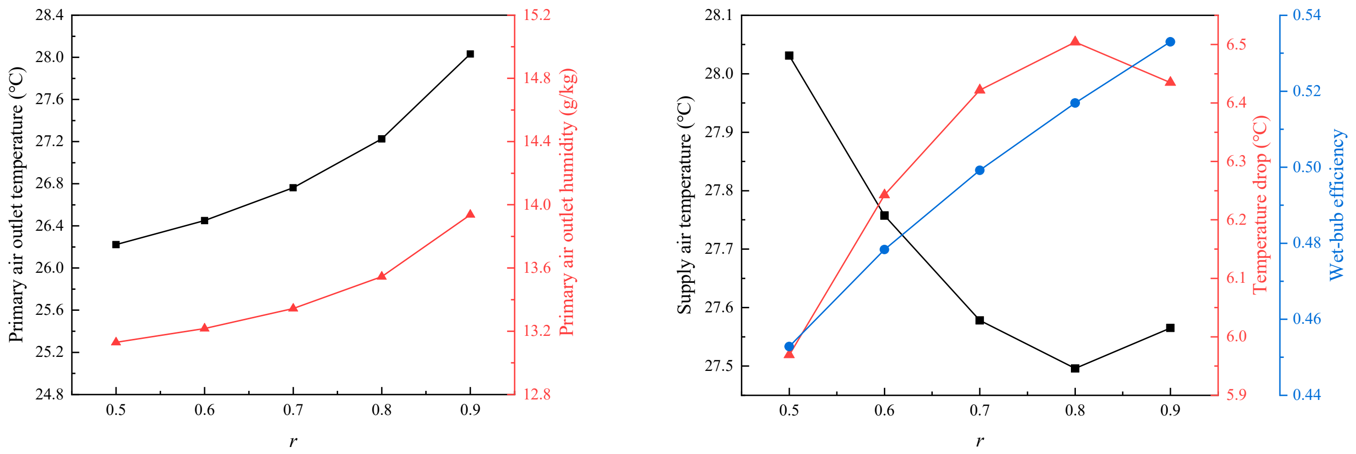

(**a**) (**b**)

Figure 7. Effect of primary air to secondary air ratio on the thermal performance of (**a**) first-stage LD-IEC, (**b**) second-stage IEC.

In contrast to the consistent trends observed in the previous parameters, Figure 7b presents a more complex relationship when it comes to the supply air temperature as r increases. It is seen that as the r value increases from 0.5 to 0.8, the supply air temperature gradually decreases, albeit at a reduced rate. However, the supply air temperature tends to grow when r is greater than 0.8. Correspondingly, the temperature drop generated by the second-stage IEC initially increases from approximately 6.0 °C to 6.5 °C, and then slightly decreases to 6.4 °C. This phenomenon can be explained by the fact that although the outlet temperature of the first-stage LD-IEC increases with an increase in the r value, the primary air from the LD-IEC serves as the secondary air for the second-stage IEC. An increase in the r value implies an increase in the flow rate entering the secondary channel of the IEC. With a constant channel spacing, a larger flow rate results in a higher convective heat and mass transfer, allowing the supply air temperature of the IEC to continue decreasing until an r value of 0.8. However, as the wet-bulb temperature also increases, its influence on the supply air temperature gradually becomes greater than the effect of the increased convective heat transfer coefficient, ultimately leading to an increase in the supply air temperature. An essential insight from this analysis is that optimizing the r value is critical to maintaining the cooling performance of the proposed system. A value that is too high may lead to less effective cooling, as demonstrated by the supply air temperature increasing beyond the optimal range for r values greater than 0.8.

In the analysis of this parameter, the supply air temperature exceeds 27 °C, indicating the need for supplementary cooling to ensure the desired supply air temperature. Regarding the wet-bulb temperature of the IEC, Figure 7b shows a significant increase in wet-bulb efficiency from 0.453 to 0.533 as the r value increases.

4.4. Effect of the Solution Concentration

Figure 8 presents the influence of variations in the concentration of the desiccant solution (σ) sprayed in the primary air channel of the LD-IEC on the system's thermal performance. As the concentration becomes stronger, the difference in vapor pressure between the air–liquid interface and the main moist airstream increases, creating a larger gradient and facilitating moisture migration in the humid air. Consequently, the outlet temperature and humidity of the LD-IEC decrease as the concentration of the desiccant solution increases. In Figure 8a, it is observed that an increase in σ from 0.2 to 0.4 corresponds to a decrease in the outlet temperature and humidity of the primary air of the LD-IEC from 27.7 °C to 26.2 °C and from 17.24 g/kg to 11.30 g/kg, respectively. Moreover, the wet-bulb temperature of the air processed by the LD-IEC decreases from the inlet temperature of 27.1 °C to a range of 19.5–24 °C. As the temperature and humidity of the primary air from the LD-IEC (which serves as the secondary air for the second-stage IEC) decrease, the supply air temperature of the second-stage IEC increases from 28.9 °C to 26.9 °C, and the cooling ability of the IEC for the primary air increases from 5.1 °C to 7.1 °C. When σ reaches 0.4, the IEC's supply air temperature falls below 27 °C, indicating that supplementary cooling can be suspended at this point. This implies that at higher σ values, the multi-stage IEC system could potentially meet the cooling requirements without the need for additional cooling methods. It is important to mention that the regeneration of the desiccant solution, which involves restoring the diluted solution that has absorbed moisture from the humid air, requires a dedicated regeneration device. This ensures a continuous and stable humidity gradient between the primary air and the solution surface. The regeneration process can utilize waste heat or solar thermal energy, and further investigation will be conducted in future research to optimize this aspect. The discussion of solution regeneration is beyond the scope of this paper. Regarding the wet-bulb temperature of the IEC, it is seen from Figure 8b that as the concentration becomes stronger, the wet-bulb efficiency slightly decreases from 0.513 to 0.491.

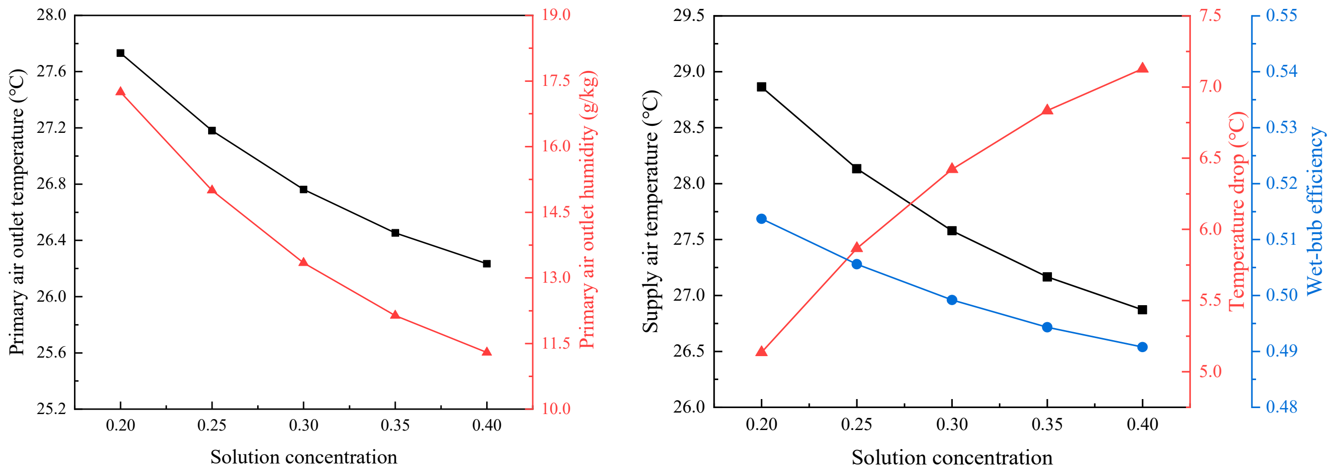

(**a**) (**b**)

Figure 8. Effect of solution concentration on the thermal performance of (**a**) first-stage LD-IEC, (**b**) second-stage IEC.

4.5. Effect of Temperature of Circulated Air from the DC

Figure 9 presents the impact of variations in the inlet air temperature of the second-stage IEC's primary air channel on the system's thermal performance. The impetus for this investigation stems from the fluctuating air temperatures in the DC, attributable to heat emissions from electronic components, which are influenced by factors such as the DC size, energy-saving requirements, and density of the installed equipment. Initially, the first-stage LD-IEC reduces the wet-bulb temperature of the humid air from 27.1 °C to 21.1 °C, which is then utilized as the secondary air for the second-stage IEC, significantly enhancing the IEC's cooling capacity. As the inlet temperature of the circulating air gradually increases, the outlet air temperature of the IEC also rises. Figure 9 demonstrates that when the inlet temperature increases from 32 °C to 40 °C, the IEC's outlet air temperature increases from

26.6 °C to 30.4 °C, resulting in an increase in the IEC's cooling capacity for the primary air from 5.4 °C to 9.7 °C. Upon the circulating air temperature surpassing 32 °C, the outlet air temperature of the second-stage IEC exceeds 27 °C, signifying the requisition of auxiliary cooling to attain the prescribed supply air temperature for DCs. Regarding the wet-bulb temperature of the IEC, Figure 9 shows a slight increase in wet-bulb efficiency from 0.495 to 0.510 as the temperature of the circulating air rises.

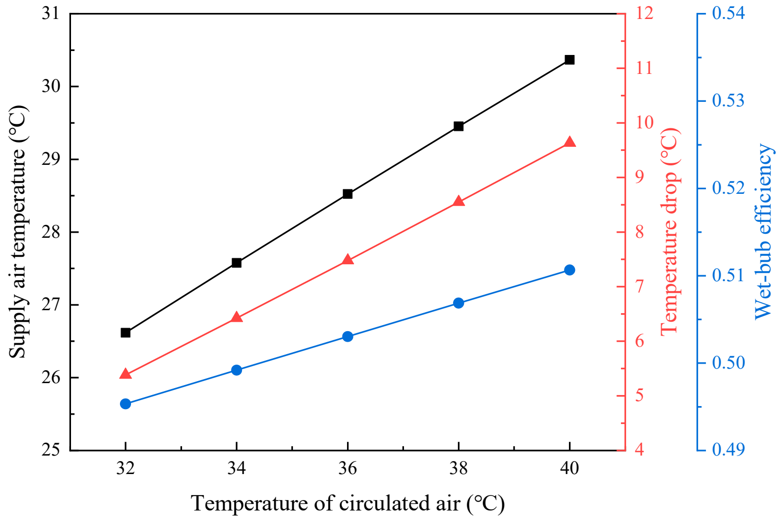

Figure 9. Influence of temperature of circulated air from the DC on the thermal performance of second-stage IEC.

4.6. Effect of Velocity of Circulated Air from the DC

Figure 10 illustrates the effect of variations in the air velocity of the second-stage IEC's primary air channel on the system's thermal performance. Since the velocity of the second-stage IEC does not impact the air treatment process of the first-stage LD-IEC, as discussed in the previous section, the first-stage LD-IEC significantly reduces the wet-bulb temperature of the inlet humid air to 21.1 °C, which serves as the secondary air for the second-stage IEC. It is observed that as the velocity of the primary channel of the second-stage IEC increases, the outlet air temperature of the IEC also grows. If the air is accelerated from 2 m/s to 4 m/s, the IEC's outlet air temperature rises from 25.5 °C to 27.4 °C. This inversely affects the IEC's temperature drop of the primary air from 6.5 °C to 4.6 °C. Although an increase in velocity enhances convective heat transfer, it also raises the mass flow rate, and the latter has a more significant effect, leading to an increase in the temperature of the supply air as the circulated air velocity increases. When the air velocity in the channel exceeds 3.5 m/s, the IEC's outlet air temperature surpasses 27 °C, indicating the need to activate supplementary cooling to meet the desired supply air temperature for data centers. Regarding the wet-bulb temperature of the IEC, Figure 10 demonstrates a rapid increase in wet-bulb efficiency from 0.602 to 0.424 as the air velocity rises. This efficiency upsurge is predominantly ascribed to the intensified air flow, which, despite enhancing convective heat transfer to a certain degree, primarily leads to a notable temperature increment. Thus, the primary air velocity in the IEC should be carefully considered in practical engineering projects.

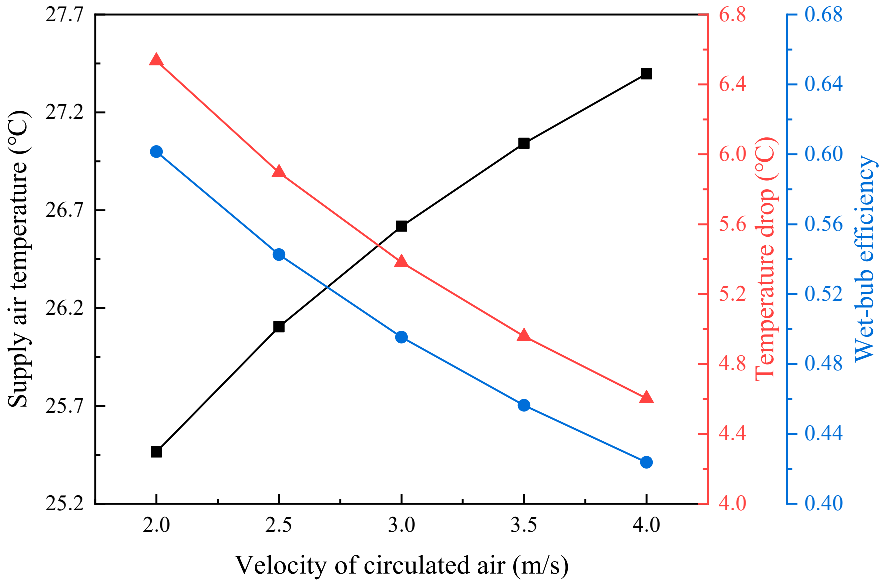

Figure 10. Effect of velocity of circulated air from the DC on the thermal performance of second-stage IEC.

4.7. Case Study for the Application in a Hot and Humid Region

As mentioned in the previous section, the integration of the liquid desiccant in the IEC system mitigates the detrimental effects of high ambient humidity levels on the evaporation process, particularly within hot and humid climates. To present the annual feasibility of employing the multi-stage IEC system, Hong Kong's weather conditions in the typical meteorological year (TMY) are input as the primary air of the LD-IEC. According to the existing literature on the AC operation status of the typical DC, the circulated air after removing the heat from the IT equipment can be determined as 34 °C. In addition, the recommended range of supply air temperature to the electronic equipment zone is from 18 °C to 27 °C.

Figure 11 presents the supply air temperature of a single IEC and the proposed IEC system given the outdoor air conditions in Hong Kong. When the multi-stage IECs or the single IEC cannot handle the circulated air to the required temperature (27 °C), the rest of the cooling load will be treated by the supplementary cooling section, and the operating hour is counted. As shown in Figure 11, both the standalone IEC system and the multi-stage IEC system demonstrate effective cooling of circulating air when outdoor temperatures and humidity are relatively low, such as in early spring, late autumn, and winter. However, the cooling capacity of the single IEC diminishes greatly during the summer months due to the severe constraints imposed by high outdoor temperatures and humidity on water evaporation. The average temperature drop is only 5.5 °C in summer, which is much lower than the annual average temperature drop of 8.7 °C. The number of hours exceeding the upper temperature limit (27 °C) reaches as high as 3550 h, necessitating prolonged operation of supplementary cooling equipment, particularly in the summer. Furthermore, for engineering projects where the supply air temperature is designed to be 25 °C, this would significantly increase the operational time of supplementary cooling equipment to 5092 h annually. In comparison to a single IEC, this system benefits from the incorporation of an LD-IEC, which provides a lower wet-bulb temperature for the secondary air used in the IEC. Consequently, this enables the IEC to consistently reduce the supply air temperature to below 27 °C. During the summer months, the system achieves an average temperature difference of 9.5 °C, which is improved by 72.7% compared to that of the standalone IEC. The annual average temperature drop is 11.5 °C, both of which are significantly superior to a standalone IEC system. Given that the supplementary cooling module is activated if the supply air exceeds 25 °C, this multi-stage IEC system reduces the operational hours of the supplementary cooling module to a mere 31 h per year, substantially cutting down the runtime of the supplementary cooling system. This advancement represents a significant stride toward the goal of relying solely on passive cooling methods for DC cooling.

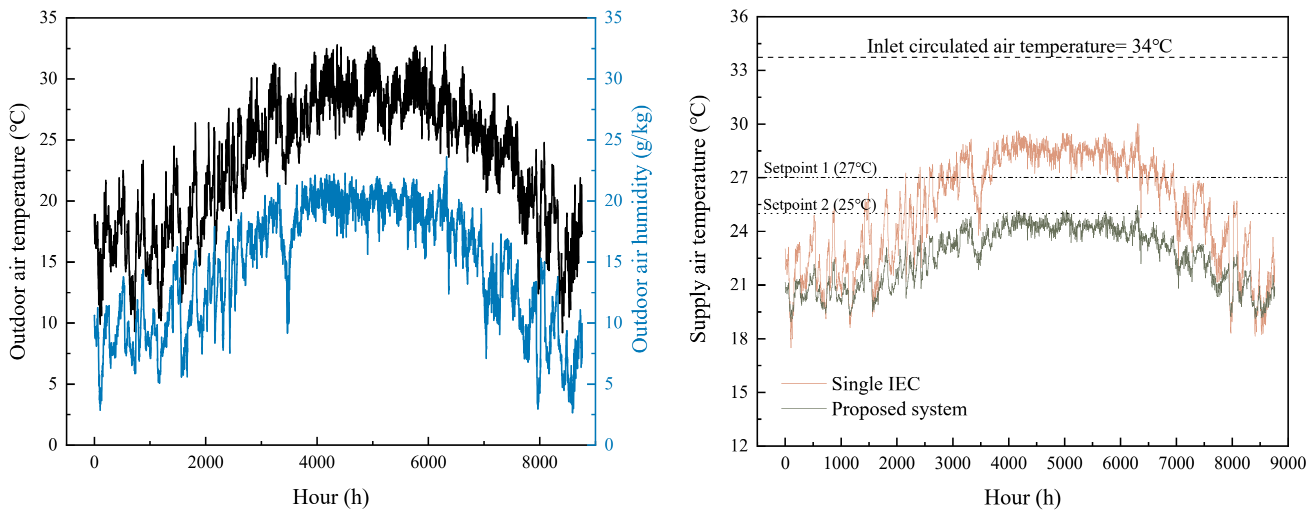

(**a**) (**b**)

Figure 11. Profile of (**a**) outdoor air status in Hong Kong, (**b**) supply air temperature of the proposed system.

4.8. Discussions

In hot and humid regions, the interaction between the primary air temperature and humidity with the system's outlet conditions underscores the reliance of evaporative cooling processes on ambient air properties. The increased temperature and RH challenge the cooling performance due to the diminished humidity gradient between the air and the wet surfaces within the IEC. The LD-IEC's role in pre-treating the air before it enters the second-stage IEC is instrumental in enhancing the overall thermal performance. By reducing the humidity, the first-stage LD-IEC effectively lowers the wet-bulb temperature of the air, which is an essential factor of the evaporative cooling potential. The mass flow ratio (r) emerges as a critical parameter, with an optimal range necessary to balance the cooling efficiency against the system's cooling performance. The desiccant solution concentration (σ) dictates the dehumidification strength and the subsequent cooling potential as well. Regarding the second-stage IEC, inlet circulated air temperature from the DC and the channel velocity influence the cooling capacity, where increased air temperatures can improve the IEC's temperature drop and wet-bulb efficiency. The elevated air velocity can improve the convective heat transfer, but the increased mass flow rate is the predominant factor that ultimately leads to higher outlet temperatures. Lastly, the case study involving Hong Kong's climatic conditions indicates that the multi-stage IEC system's ability to maintain the supply air temperature within the desired threshold for the majority of the year marks a substantial improvement over conventional single-stage IEC systems, which offers insights into the system's annual operational feasibility and demonstrates the system's capability in reducing the reliance on the energy-intensive traditional cooling system for DCs in hot and humid regions.

Table 2 presents a comparison between recent studies on hybrid IEC systems and this study. Currently, a few composite systems related to DCs are reported, especially in hot and humid regions. In hot and arid regions, both the primary and secondary air for IEC can be sourced from outdoors, as the lower wet-bulb temperature outside makes it possible for a single-stage IEC to achieve the required supply air temperature. However, in hot and humid regions, the high outdoor humidity significantly limits the effectiveness of evaporative cooling. Therefore, some researchers propose to utilize exhaust air from air-conditioned spaces as the secondary air to enhance the cooling effect of the IEC [23,25]. However, for buildings with specialized uses such as DCs which typically involve air recirculating between the indoor space and air handling units without fresh air [30], the source of secondary air can only be from outdoors, and this outdoor air needs to be pre-treated to reduce its humidity and wet-bulb temperature before it can be used as the secondary air in the second-stage IEC. Hence, this study has proposed the LD-IEC to achieve this purpose. Compared to existing studies, the achieved temperature drop is satisfactory, demonstrating the potential of using this system in hot and humid regions.

Table 2. Comparison with the published studies.

Research	**Nemati et al. [24]**	**Hu et al. [29]**	**Wan et al. [23]**	**Present Study**
Type of IEC	Counter flow	Counter flow	Counter flow	Cross flow
IEC size (L × H, m^2)	0.5 × 0.5	1 × 1	0.6 × 0.15	0.6 × 0.6
System configuration	Earth-air heat exchanger + IEC	RC + IEC	IEC + cooling coil	LD-IEC + IEC
Building type	Residential building	Residential building	Commercial building	Data center
Climate region	Hot and arid	Hot and arid	Hot and humid	Hot and humid
Working air source	Outdoor space	Outdoor space	Indoor AC space	Outdoor space
Temperature drop (°C)	4.2	8.8	10	9.5

In addition to being a technical solution to DC cooling in hot-humid regions, this study may be possible to motivate the update of some policies related to IECs and DCs. Firstly, IEC systems are originally suitable for use in arid and hot regions. However, the results mentioned above have demonstrated that with the assistance of a desiccant solution, a composite IEC system can be effectively applied in hot and humid areas. Consequently, policies can encourage the adoption of IEC systems in DCs within hot and humid regions, supplemented by the liquid desiccant described in this paper (i.e., spraying the desiccant solution in the primary air channel in the first stage). In addition, DCs are typically low-rise buildings with ample roof area. Policies can suggest making full use of the rooftop space to install solar energy equipment for regeneration of the desiccant solution or even power supply to such IEC systems.

5. Limitations and Future Works

This study has conceptually proposed a multi-stage system and analyzed its thermal performance for data center (DC) cooling in hot and humid climates. Nevertheless, the system's integration remains unrealized in the laboratory in reality. The detailed approach for regenerating the liquid desiccant—a critical component of the system—has not been included in this research. The strategies to incorporate renewable energy such as solar energy are not presented as well. Furthermore, the integrated system is not optimized to contribute a better cooling performance. Additionally, a comprehensive economic analysis, which would include the determination of potential economic benefits and payback periods, is requisite for practical engineering applications. Therefore, future works will be carried out based on the above limitations: (1) To assemble the multi-stage IEC on the laboratory scale or in a pilot-scale setting; (2) To incorporate the liquid desiccant regeneration system for further investigation; (3) To involve a renewable energy system to enhance the low-carbon and sustainability aspects; (4) To optimize the proposed system for optimal operating conditions; (5) To carry out an economic analysis to estimate the system's cost effectiveness, operational expenses, and return on investment.

6. Conclusions

In this study, a multi-stage IEC system was developed for the cooling of data centers (DCs) situated in hot and humid regions. Liquid desiccant (LD) was incorporated into the first-stage IEC to mitigate the influence of high-humidity ambient air on the cooling performance and expand the application range of the IEC technology. The model of the proposed system was constructed with validation from the published literature, and the parametric analysis was carried out to investigate the thermal performance under various inlet conditions. Furthermore, a case study was conducted based on a typical hot-humid climatic zone (Hong Kong) to demonstrate the feasibility of the proposed system for achieving the required supply air temperature for a DC. The main findings are summarized as follows.

(1) The first-stage LD-IEC effectively reduces the wet-bulb temperature of the ambient air, thereby enhancing the cooling performance of the second-stage IEC. However, a higher ambient air temperature, relative humidity, and circulated air velocity may diminish the temperature drop, while an increased solution concentration and circulated air temperature can expand the temperature drop.
(2) The cooling performance of the system improves with an increasing mass flow ratio up to 0.8, but experiences a reduction as the mass flow ratio continues to grow to 0.9. This highlights the importance of determining the optimal value during the design stage.
(3) The case study illustrates that the multi-stage IEC system can alleviate the constraints of high-humidity ambient air on the cooling effect compared to a single IEC, which greatly improves the temperature drop by 72.7%. This results in a significant reduction in the operation time of energy-intensive supplementary cooling equipment from 5092 h to 31 h given the supply air temperature threshold of 25 °C. This advancement brings us closer to the goal of utilizing fully natural passive cooling technology for the cooling of DCs in hot and humid regions.
(4) Future works should include the integration of the multi-stage IEC in real practice, the combination of the liquid desiccant regeneration system and a renewable energy system, optimization, and economic analysis, which should demonstrate the reliable cooling, energy saving, and cost-friendliness of the proposed system in DCs of hot-humid regions.

Author Contributions: Conceptualization, methodology, programming, formal analysis, writing—original draft: W.S.; validation, data curation, resources: X.M.; conceptualization, methodology, writing—review & editing: Y.M.; supervision, funding acquisition, writing—review & editing: H.Y. All authors have read and agreed to the published version of the manuscript.

Funding: This research work was supported by the National Natural Science Foundation of China (No. 52208111). This work was also supported by the PolyU Distinguished Postdoctoral Fellowship Scheme (1-YWDD).

Institutional Review Board Statement: Not applicable.

Informed Consent Statement: Not applicable.

Data Availability Statement: The data presented in this study are available on request from the corresponding author.

Conflicts of Interest: The authors declare that they have no known competing financial interests or personal relationships that could have appeared to influence the work reported in this paper.

Nomenclature

c_{pa}	Specific heat of air, J/(kg·°C)
d	Channel height, mm
d_e	Hydraulic diameter of channel, m
h	Heat transfer coefficient, W/(m^2·°C)
h_m	Mass transfer coefficient, kg/(m^2·s)
h_{fg}	Heat capacity of vaporization, 2501 kJ/kg
H	Height, m
i	Specific enthalpy, kJ/kg
L	Length, m
Le	Lewis number
m	Mass flow rate of air, kg/s
Nu	Nusselt number
P	Pressure, kPa
Pr	Prandtl number
r	Mass flow ratio
Re	Reynolds number
t	Temperature, °C
u	Air velocity, m/s
w	Humidity ratio, g/kg
Greek symbols	
σ	Solution concentration
λ	Thermal conductivity, W/(m·°C)
Abbreviation	
AC	Air conditioning
DC	Data center
LD-IEC	Liquid desiccant-based indirect evaporative cooling
IEC	Indirect evaporative cooling
RH	Relative humidity
Subscripts	
amb	Ambient air
atm	Atmospheric
circ	Circulated air
d	Dehumidification
e	Evaporation
p	Primary air
s	Secondary air
sat	Saturated status
sol	Solution
w	Water film
in	Inlet
out	Outlet

References

1. Fan, J.L.; Li, Z.; Huang, X.; Li, K.; Zhang, X.; Lu, X.; Wu, J.; Hubacek, K.; Shen, B. A net-zero emissions strategy for China's power sector using carbon-capture utilization and storage. *Nat. Commun.* **2023**, *14*, 5972. [CrossRef]
2. Lai, L.; Wang, X.; Hu, E.; Choon Ng, K. A vision of dew point evaporative cooling: Opportunities and challenges. *Appl. Therm. Eng.* **2024**, *244*, 122683. [CrossRef]
3. Liu, X.; Liu, X.; Jiang, Y.; Zhang, T.; Hao, B. Photovoltaics and Energy Storage Integrated Flexible Direct Current Distribution Systems of Buildings: Definition, Technology Review, and Application. *CSEE J. Power Energy Syst.* **2023**, *9*, 829–845. [CrossRef]
4. Chen, J.; Gong, Q.; Lu, L. Evaluation of passive envelope systems with radiative sky cooling and thermally insulated glazing materials for cooling. *J. Clean. Prod.* **2023**, *398*, 136607. [CrossRef]
5. Ma, X.; Zeng, C.; Zhu, Z.; Zhao, X.; Xiao, X.; Akhlaghi, Y.G.; Shittu, S. Real life test of a novel super performance dew point cooling system in operational live data centre. *Appl. Energy* **2023**, *348*, 121483. [CrossRef]
6. Zhang, Y.; Shan, K.; Li, X.; Li, H.; Wang, S. Research and Technologies for next-generation high-temperature data centers—State-of-the-arts and future perspectives. *Renew. Sustain. Energy Rev.* **2023**, *171*, 112991. [CrossRef]

7. Liu, Y.; Yang, X.; Li, J.; Zhao, X. Energy savings of hybrid dew-point evaporative cooler and micro-channel separated heat pipe cooling systems for computer data centers. *Energy* **2018**, *163*, 629–640. [CrossRef]
8. Zhang, Y.; Zhao, Y.; Dai, S.; Nie, B.; Ma, H.; Li, J.; Miao, Q.; Jin, Y.; Tan, L.; Ding, Y. Cooling technologies for data centres and telecommunication base stations—A comprehensive review. *J. Clean. Prod.* **2022**, *334*, 130280. [CrossRef]
9. Faraji, H.; Alami, M.E.; Arshad, A.; Hariti, Y. Numerical Survey on Performance of Hybrid NePCM for Cooling of Electronics: Effect of Heat Source Position and Heat Sink Inclination. *J. Therm. Sci. Eng. Appl.* **2021**, *13*, 4049431. [CrossRef]
10. Faraji, H.; Yıldız, Ç.; Arshad, A.; Arıcı, M.; Choukairy, K.; El Alami, M. Passive thermal management strategy for cooling multiple portable electronic components: Hybrid nanoparticles enhanced phase change materials as an innovative solution. *J. Energy Storage* **2023**, *70*, 108087. [CrossRef]
11. Kabeel, A.E.; Bassuoni, M.M.; Abdelgaied, M. Experimental study of a novel integrated system of indirect evaporative cooler with internal baffles and evaporative condenser. *Energy Convers. Manag.* **2017**, *138*, 518–525. [CrossRef]
12. De Antonellis, S.; Joppolo, C.M.; Liberati, P. Performance measurement of a cross-flow indirect evaporative cooler: Effect of water nozzles and airflows arrangement. *Energy Build.* **2019**, *184*, 114–121. [CrossRef]
13. Kim, H.-J.; Ham, S.-W.; Yoon, D.-S.; Jeong, J.-W. Cooling performance measurement of two cross-flow indirect evaporative coolers in general and regenerative operation modes. *Appl. Energy* **2017**, *195*, 268–277. [CrossRef]
14. Shi, W.; Yang, H.; Ma, X.; Liu, X. Performance prediction and optimization of cross-flow indirect evaporative cooler by regression model based on response surface methodology. *Energy* **2023**, *283*, 128636. [CrossRef]
15. Kabeel, A.E.; Abdelgaied, M. Numerical and experimental investigation of a novel configuration of indirect evaporative cooler with internal baffles. *Energy Convers. Manag.* **2016**, *126*, 526–536. [CrossRef]
16. Cui, X.; Yang, C.; Yan, W.; Zhang, L.; Wan, Y.; Chua, K.J. Experimental study on a moisture-conducting fiber-assisted tubular indirect evaporative cooler. *Energy* **2023**, *278*, 128014. [CrossRef]
17. Xiao, X.; Liu, J. A state-of-art review of dew point evaporative cooling technology and integrated applications. *Renew. Sustain. Energy Rev.* **2024**, *191*, 114142. [CrossRef]
18. Ma, X.; Shi, W.; Yang, H. Spray parameter analysis and performance optimization of indirect evaporative cooler considering surface wettability. *J. Build. Eng.* **2024**, *82*, 108175. [CrossRef]
19. Sun, T.; Huang, X.; Chen, Y.; Zhang, H. Experimental investigation of water spraying in an indirect evaporative cooler from nozzle type and spray strategy perspectives. *Energy Build.* **2020**, *214*, 109871. [CrossRef]
20. Shi, W.; Yang, H.; Ma, X.; Liu, X. A novel indirect evaporative cooler with porous media under dual spraying modes: A comparative analysis from energy, exergy, and environmental perspectives. *J. Build. Eng.* **2023**, *2023*, 106874. [CrossRef]
21. Golizadeh Akhlaghi, Y.; Badiei, A.; Zhao, X.; Aslansefat, K.; Xiao, X.; Shittu, S.; Ma, X. A constraint multi-objective evolutionary optimization of a state-of-the-art dew point cooler using digital twins. *Energy Convers. Manag.* **2020**, *211*, 112772. [CrossRef]
22. Al-Zubaydi, A.Y.T.; Hong, G. Experimental study of a novel water-spraying configuration in indirect evaporative cooling. *Appl. Therm. Eng.* **2019**, *151*, 283–293. [CrossRef]
23. Wan, Y.; Huang, Z.; Soh, A.; Jon Chua, K. On the performance study of a hybrid indirect evaporative cooling and latent-heat thermal energy storage system under commercial operating conditions. *Appl. Therm. Eng.* **2023**, *221*, 119902. [CrossRef]
24. Nemati, N.; Omidvar, A.; Rosti, B. Performance evaluation of a novel hybrid cooling system combining indirect evaporative cooler and earth-air heat exchanger. *Energy* **2021**, *215*, 119216. [CrossRef]
25. Shi, W.; Yang, H.; Ma, X.; Liu, X. Techno-economic evaluation and environmental benefit of hybrid evaporative cooling system in hot-humid regions. *Sustain. Cities Soc.* **2023**, *2023*, 104735. [CrossRef]
26. Chen, Q.; Kum Ja, M.; Burhan, M.; Akhtar, F.H.; Shahzad, M.W.; Ybyraiymkul, D.; Ng, K.C. A hybrid indirect evaporative cooling-mechanical vapor compression process for energy-efficient air conditioning. *Energy Convers. Manag.* **2021**, *248*, 114798. [CrossRef]
27. Yan, H.; Chen, Y.; Min, Y.; Pan, Y. An adaptive controller based dynamic simulation of household air-conditioner with indirect evaporative cooler as dedicated outdoor air system. *Energy Build.* **2022**, *274*, 112454. [CrossRef]
28. Tripathi, R.J.; Kumar, D. Performance assessment of solar-driven indirect evaporative cooling with a novel wet channel: An experimental study. *J. Build. Eng.* **2023**, *78*, 107674. [CrossRef]
29. Hu, M.; Seng Lee, P. Performance evaluation of a passive air conditioning module integrating radiative sky cooling and indirect evaporative cooling. *Appl. Therm. Eng.* **2024**, *2024*, 122608. [CrossRef]
30. Chu, J.; Huang, X. Research status and development trends of evaporative cooling air-conditioning technology in data centers. *Energy Built Environ.* **2023**, *4*, 86–110. [CrossRef]
31. Li, C.; Mao, R.; Wang, Y.; Zhang, J.; Lan, J.; Zhang, Z. Experimental study on direct evaporative cooling for free cooling of data centers. *Energy* **2024**, *288*, 129889. [CrossRef]
32. Mohammed, R.H.; El-Morsi, M.; Abdelaziz, O. Indirect evaporative cooling for buildings: A comprehensive patents review. *J. Build. Eng.* **2022**, *50*, 104158. [CrossRef]
33. Heiliger, J. Building efficient data centers with the open compute project. In *Facebook Engineering Notes*; 2011. Available online: https://engineering.fb.com/2011/04/07/data-center-engineering/building-efficient-data-centers-with-the-open-compute-project/ (accessed on 25 February 2024).
34. Finch, P.; ENG, C. Indirect Evaporative Cooling Drives Data Center Efficiency. *ASHRAE J.* **2020**, *62*, 40–47.

35. Yan, W.; Cui, X.; Zhao, M.; Meng, X.; Yang, C.; Zhang, Y.; Liu, Y.; Jin, L. Multi-objective optimization of dew point indirect evaporative coolers for data centers. *Appl. Therm. Eng.* **2024**, *241*, 122425. [CrossRef]
36. Cui, X.; Yang, C.; Yan, W.; Wang, X.; Liu, Y.; Jin, L. Climatic applicability of indirect evaporative cooling strategies for data centers in China. *J. Build. Eng.* **2024**, *83*, 108431. [CrossRef]
37. Mumtaz, M.; Pamintuan, B.C.; Fix, A.J.; Braun, J.E.; Warsinger, D.M. Hybrid membrane dehumidification and dewpoint evaporative cooling for sustainable air conditioning. *Energy Convers. Manag.* **2023**, *294*, 117547. [CrossRef]
38. Anisimov, S.; Pandelidis, D.; Danielewicz, J. Numerical analysis of selected evaporative exchangers with the Maisotsenko cycle. *Energy Convers. Manag.* **2014**, *88*, 426–441. [CrossRef]
39. Adam, A.; Han, D.; He, W.; Amidpour, M.; Zhong, H. Numerical investigation of the heat and mass transfer process within a cross-flow indirect evaporative cooling system for hot and humid climates. *J. Build. Eng.* **2022**, *45*, 103499. [CrossRef]
40. Zheng, B.; Guo, C.; Chen, T.; Shi, Q.; Lv, J.; You, Y. Development of an experimental validated model of cross-flow indirect evaporative cooler with condensation. *Appl. Energy* **2019**, *252*, 113438. [CrossRef]
41. Cui, X.; Islam, M.R.; Mohan, B.; Chua, K.J. Theoretical analysis of a liquid desiccant based indirect evaporative cooling system. *Energy* **2016**, *95*, 303–312. [CrossRef]
42. Zhang, H.; Ma, H.; Ma, S.; Yang, M. Investigation on the performance of an indirect evaporative cooling system integrated with liquid dehumidification. *Energy Build.* **2021**, *251*, 111356. [CrossRef]
43. Zhang, Y.; Zhang, H.; Yang, H.; Chen, Y.; Leung, C.W. Counter-crossflow indirect evaporative cooling-assisted liquid desiccant dehumidifier: Model development and parameter analysis. *Appl. Therm. Eng.* **2022**, *217*, 119231. [CrossRef]
44. Min, Y.; Chen, Y.; Yang, H. Numerical study on indirect evaporative coolers considering condensation: A thorough comparison between cross flow and counter flow. *Int. J. Heat Mass Transf.* **2019**, *131*, 472–486. [CrossRef]